Using an instrumented tractor-trailer to detect damage in bridges

Eugene J. OBrien, UCD School of Civil, Structural and Environmental Engineering, Newstead Building, Belfield Campus, Dublin 4, Ireland.
Jennifer Keenahan, UCD School of Civil, Structural and Environmental Engineering, Newstead Building, Belfield Campus, Dublin 4, Ireland.

Abstract
This paper investigates an alternative to Structural Health Monitoring (SHM) which involves no sensors on the bridge itself. It uses a vehicle fitted with accelerometers on its axles as a method of monitoring the dynamic behavior of the bridge, which in turn gives an indication of the bridge's structural condition. The concept, known as 'drive by' bridge inspection, may be of particular value after an extreme event, such as an earthquake or a flood, where a rapid indication of bridge condition is needed. In the paper, a two dimensional numerical model is described of a 3-axle truck towing a half-car trailer. The vehicle-bridge dynamic interaction is modeled to test the effectiveness of the approach in identifying the structural damping of the bridge. The damping of the bridge is used here as an indicator of damage. The accelerations in the two axles of the trailer are subtracted to remove the effect of the road profile. Results indicate that the algorithm is not sensitive to transverse position of the vehicle on the bridge.

Key Words: Bridge Monitoring, Bridges, Damage Detection Models

1. Introduction

The task of detecting damage in bridges traditionally consists of visual inspections. These however are labor intensive and are often an unreliable way of determining the true condition. Recently there has been a move towards sensor based analysis of bridge condition. Existing monitoring techniques involve the direct instrumentation of the structure – commonly referred to as Structural Health Monitoring (SHM) [1–3]. More recently, a small number of authors have shifted to the instrumentation of a vehicle, rather than the bridge, which can be less expensive and less time-consuming. This approach is referred to as 'drive-by' bridge inspection [4]. The feasibility of detecting frequencies from the dynamic response of an instrumented vehicle passing over a bridge has been verified theoretically by Yang et al. [5], in field trials [6, 7] and in laboratory investigations [4, 8-10]. As an alternative to detecting changes in frequency, Yabe and Miyamoto [11] use the mean displacement of the rear axle of a city bus passing over a bridge a large number of times as a damage indicator. Kim et al. [12] construct scaled Vehicle Bridge Interaction (VBI) laboratory experiments and consider the use of autoregressive coefficients as a damage indicator. The analysis of damping has been considered to a lesser extent [13]. However, recent evidence suggests that damping is quite sensitive to damage in structural elements and in some cases, more sensitive than other indicators [14, 15].

This paper describes a novel approach that uses a truck-trailer vehicle system, fitted with accelerometers on the trailer axles, to detect changes in the damping of a bridge which would indicate deterioration of the bridge's condition. The concept is that the relatively heavy truck dynamically excites the bridge while sensors in the trailer are used to monitor the resulting vibrations. For numerical simulations, a VBI model is created in Matlab. The trailer axles are assigned identical properties – as can easily be the case with a simple trailer. The axle accelerations from the front and rear axles of the trailer are *subtracted* from one another. Each trailer axle is excited by the same road profile and by an element of bridge vibration at a different point in time. Subtracting the signals, time shifted by the interval between axle arrivals, has the effect of removing most of the influence of the road profile. This is a key feature of this approach and is the reason why the results are better than in simpler drive-by monitoring concepts. The vehicle is simulated crossing different paths through the road profile to assess sensitivity to transverse position of the vehicle on the bridge.

2. Vehicle-Bridge Interaction Model

The truck-trailer model can be seen in Fig. 1. The truck is a three axle, five-degree-of-freedom rigid vehicle. The five degrees-of-freedom account for the axle hop displacements of each of the three axles, $y_{u,i}$ (i = 1,2,3), sprung mass bounce displacement, $y_{s,1}$, and sprung mass pitch rotation, $\theta_{s,1}$. The body of the vehicle is represented by the sprung mass, $m_{s,1}$, and the axle components are represented by the unsprung masses, $m_{u,1}$, $m_{u,2}$ and $m_{u,3}$ respectively. The axle masses connect to the road surface via springs of stiffness $K_{t,1,}$ $K_{t,2}$ and $K_{t,3}$, while the body mass is connected to the tyres by springs of stiffness $K_{s,1}$, $K_{s,2}$ and $K_{s,3}$ with viscous dampers of value $C_{s,1}$, $C_{s,2}$ and $C_{s,3}$. This combination represents the suspension of the truck system.

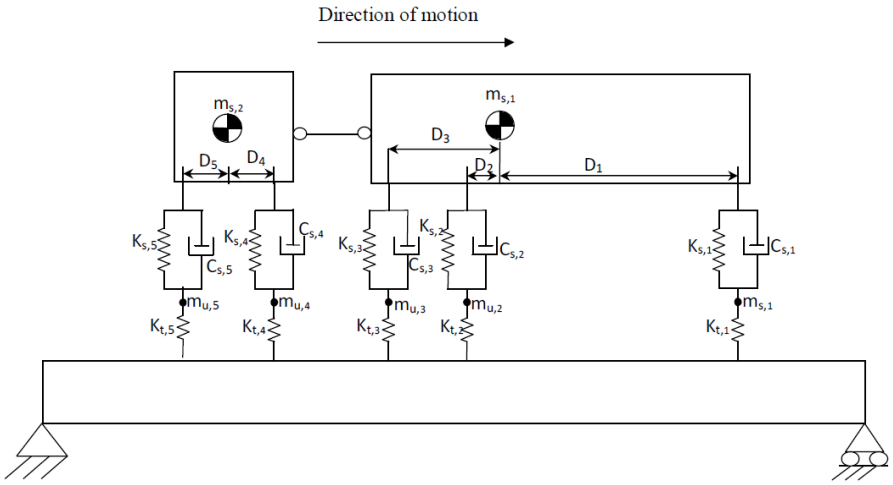

Fig. 1: Truck-Trailer Model

The trailer is a two axle, four-degree-of-freedom half-car suspension model. The four degrees-of-freedom account for axle hop displacements of each of the two axles, $y_{u,i}$ ($i = 4,5$), sprung mass bounce displacement, $y_{s,2}$ and sprung mass pitch rotation, $\theta_{s,2}$. The body of the vehicle is represented by the sprung mass, $m_{s,2}$, and the axle components are represented by the unsprung masses, $m_{u,4}$ and $m_{u,5}$. The suspension springs have stiffness $K_{t,4}$ and $K_{t,5}$, while the tyres springs have stiffness $K_{s,4}$ and $K_{s,5}$. The viscous dampers have coefficients, $C_{s,4}$ and $C_{s,5}$. Tyre damping is assumed to be negligible here for both the tractor and trailer and is thus omitted. The model also accounts for the sprung mass moments of inertia $I_{s,1}$ and $I_{s,2}$for the truck and trailer respectively. The centre of gravity of the truck is taken to be at two thirds the wheel base length from the front axle, and the centre of gravity of the trailer is taken to be central between the axles. The truck and trailer vehicle properties are gathered from the literature [16, 17, 18] and presented in Table 1. The geometry and mass of the truck are obtained from a manufacturer specification for a 30 t three-axle truck [19].

Table 1 Truck and Trailer Properties

Property	Unit	Truck Symbol	Truck Value	Trailer Symbol	Trailer Value
Body Mass	kg	$m_{s,1}$	27100	$m_{s,2}$	400
Axle masses	kg	$m_{u,1}$	700	$m_{u,4}$	50
		$m_{u,2}$	1100	$m_{u,5}$	50
		$m_{u,3}$	1100		
Suspension stiffness	N m^{-1}	$K_{s,1}$	4×10^5	$K_{s,4}$	4×10^5
		$K_{s,2}$	1×10^6	$K_{s,5}$	4×10^5
		$K_{s,3}$	1 x 10^6		
Suspension Damping	Ns m^{-1}	$C_{s,1}$	10×10^3	$C_{s,4}$	10×10^3
		$C_{s,2}$	20×10^3	$C_{s,5}$	10×10^3
		$C_{s,3}$	20×10^3		
Tyre Stiffness	N m^{-1}	$K_{t,1}$	1.75×10^6	$K_{t,4}$	1.75×10^6
		$K_{t,2}$	3.5×10^6	$K_{t,5}$	1.75×10^6
		$K_{t,3}$	3.5×10^6		
Moment of Inertia	kg m^2	$I_{s,1}$	1.56×10^5	$I_{s,2}$	241.67
Distance of axle to centre of gravity	m	D_1	4.57	D_4	1
		D_2	1.43	D_5	1
		D_3	3.23		
Body mass frequency	Hz	$f_{body,1}$	1.12	$f_{body,2}$	1.77
Axle mass frequency	Hz	$f_{axle,1}$	8.84	$f_{axle,4}$	33.1
		$f_{axle,2}$	10.18	$f_{axle,5}$	33.1
		$f_{axle,3}$	10.22		

The equations of motion of the vehicle are obtained by imposing equilibrium of all forces and moments acting on the vehicle and expressing them in terms of the degrees of freedom. They are given by

$$\mathbf{M_v}\ddot{\mathbf{y}}_\mathbf{v} + \mathbf{C_v}\dot{\mathbf{y}}_\mathbf{v} + \mathbf{K_v}\mathbf{y_v} = \mathbf{f_v} \quad (1)$$

where $\mathbf{M_v}$, $\mathbf{C_v}$ and $\mathbf{K_v}$ are the mass, damping and stiffness matrices of the vehicle respectively. The ($n \times 1$) vectors $\mathbf{y_v}$, $\dot{\mathbf{y}}_\mathbf{v}$ and $\ddot{\mathbf{y}}_\mathbf{v}$ contain the of vehicle displacements, their velocities and accelerations respectively. The vector $\mathbf{f_v}$ contains the time varying interaction forces applied by the vehicle to the bridge:

$$\mathbf{f_v} = \{0 \quad 0 \quad -F_{t,1} \quad -F_{t,2} \quad -F_{t,3} \quad 0 \quad 0 \quad -F_{t,4} \quad -F_{t,5}\}^{\mathrm{T}} \tag{2}$$

The term $F_{t,i}$ represents the dynamic interaction force at wheel *i* given by Eq. (3).

$$F_{t,i} = K_{t,i}(y_{u,i} - y_{br,i} - r_i); \tag{3}$$

The equations of motion of the VBI model are shown below. The nine degrees of freedom correspond to body bounce of the truck (Eq. (4)) and trailer (Eq. (5)), body pitch of the truck (Eq. (6)) and trailer (Eq. (7)), and axle hop for each of the five axles; the latter can be represented by the form given in Eq. (8). For i = 1, 4, $D_i\dot{\theta}_{s,j}$ is taken as a positive number, and for i = 2, 3, 5, $D_i\dot{\theta}_{s,j}$ is taken as negative.

$$\begin{aligned} m_{s,1}\ddot{y}_{s,1} + C_{s,1}(\dot{y}_{s,1} + D_1\dot{\theta}_{s,1} - \dot{y}_{u,1}) + K_{s,1}(y_{s,1} + D_1\theta_{s,1} - y_{u,1}) + C_{s,2}(\dot{y}_{s,1} - D_2\dot{\theta}_{s,1} \\ - \dot{y}_{u,2}) + K_{s,2}(y_{s,1} - D_2\theta_{s,1} - y_{u,2}) + C_{s,3}(\dot{y}_{s,1} - D_3\dot{\theta}_{s,1} - \dot{y}_{u,3}) \\ + K_{s,3}(y_{s,1} - D_3\theta_{s,1} - y_{u,3}) = 0 \end{aligned} \tag{4}$$

$$\begin{aligned} m_{s,2}\ddot{y}_{s,2} + C_{s,4}(\dot{y}_{s,2} + D_4\dot{\theta}_{s,2} - \dot{y}_{u,4}) + K_{s,4}(y_{s,2} + D_4\theta_{s,2} - y_{u,4}) + C_{s,5}(\dot{y}_{s,2} - D_5\dot{\theta}_{s,2} \\ - \dot{y}_{u,5}) + K_{s,5}(y_{s,2} - D_5\theta_{s,2} - y_{u,5}) = 0 \end{aligned} \tag{5}$$

$$\begin{aligned} I_{s,1}\ddot{\theta}_{s,1} + D_1\left[C_{s,1}(\dot{y}_{s,1} + D_1\dot{\theta}_{s,1} - \dot{y}_{u,1}) + K_{s,1}(y_{s,1} + D_1\theta_{s,1} - y_{u,1})\right] \\ - D_2\left[C_{s,2}(\dot{y}_{s,1} - D_2\dot{\theta}_{s,1} - \dot{y}_{u,2}) + K_{s,2}(y_{s,1} - D_2\theta_{s,1} - y_{u,2})\right] \\ - D_3\left[C_{s,3}(\dot{y}_{s,1} - D_3\dot{\theta}_{s,1} - \dot{y}_{u,3}) + K_{s,3}(y_{s,1} - D_3\theta_{s,1} - y_{u,3})\right] = 0 \end{aligned} \tag{6}$$

$$\begin{aligned} I_{s,2}\ddot{\theta}_{s,2} + D_4\left[C_{s,4}(\dot{y}_{s,2} + D_4\dot{\theta}_{s,2} - \dot{y}_{u,4}) + K_{s,4}(y_{s,2} + D_4\theta_{s,2} - y_{u,4})\right] \\ - D_5\left[C_{s,5}(\dot{y}_{s,2} - D_5\dot{\theta}_{s,2} - \dot{y}_{u,5}) + K_{s,5}(y_{s,2} - D_5\theta_{s,2} - y_{u,5})\right] = 0 \end{aligned} \tag{7}$$

$$\begin{aligned} m_{u,i}\ddot{y}_{u,i} - C_{s,i}(\dot{y}_{s,j} \pm D_i\dot{\theta}_{s,j} - \dot{y}_{u,i}) - K_{s,1}(y_{s,j} \pm D_i\theta_{s,j} - y_{u,i}) - P_i + F_{t,i} \\ = 0; \qquad i = 1,2,\ldots,5; j = 1,2 \end{aligned} \tag{8}$$

The bridge model used here is a simply supported 15 m Finite Element beam that consists of twenty discretized beam elements with four degrees of freedom. The beam therefore has a total of n = 42 degrees of freedom. It has a constant modulus of elasticity E = 3.5 × 10^{10} N m^{-2}, mass per unit length, μ = 28 125 kg m^{-1} and second moment of area, J = 0.5273 m^4. The first natural frequency of the beam is 5.65 Hz. The response of a discretized beam model to a series of moving time-varying forces is given by the system of equations:

$$\mathbf{M_b}\ddot{\mathbf{y}}_\mathbf{b} + \mathbf{C_b}\dot{\mathbf{y}}_\mathbf{b} + \mathbf{K_b}\mathbf{y_b} = \mathbf{N_b}\mathbf{f_{int}} \tag{9}$$

where $\mathbf{M_b}$, $\mathbf{C_b}$ and $\mathbf{K_b}$ are the ($n \times n$) global mass, damping and stiffness matrices of the beam model respectively and $\mathbf{y_b}$, $\dot{\mathbf{y}}_\mathbf{b}$ and $\ddot{\mathbf{y}}_\mathbf{b}$ are the ($n \times 1$) global vectors of nodal bridge displacements and rotations, their velocities and accelerations respectively. The product $\mathbf{N_b}\mathbf{f_{int}}$ is the ($n \times 1$) global vector of forces applied to the bridge nodes. The vector $\mathbf{f_{int}}$ contains the interaction forces between the vehicle and the bridge and is described using the following vector:

$$\mathbf{f_{int}} = \mathbf{P} + \mathbf{F_t} \tag{10}$$

where $\mathbf{P}$ is the static axle load vector and $\mathbf{F_t}$ contains the dynamic wheel contact forces of each axle. The matrix $\mathbf{N_b}$ is a ($n \times n_f$) location matrix that distributes the n_f applied interaction forces on beam elements to equivalent forces acting on nodes. This location matrix can be used to calculated bridge displacement under each wheel, $\mathbf{y_{br}}$:

$$\mathbf{y_{br}} = \mathbf{N_b^T}\,\mathbf{y_b} \tag{11}$$

The damping ratio of the bridge, ξ, is varied in simulations to assess the system's potential as an indicator of changes in damping. Although complex damping mechanisms may be present in the structure, viscous damping is typically used for bridge structures and is deemed to be sufficient to reproduce the bridge response accurately. Therefore, Rayleigh damping is adopted here to model viscous damping:

$$\mathbf{C_b} = \alpha\mathbf{M_b} + \beta\mathbf{K_b} \tag{12}$$

where α and β are constants. The damping ratio is assumed to be the same for the first two modes [20] and α and β are obtained from $\alpha = 2\,\xi\,\omega_1\omega_2/(\omega_1+\omega_2)$ and $\beta = 2\,\xi\,/\,(\omega_1+\omega_2)$ where ω_1 and ω_2 are the first two natural frequencies of the bridge [21].

The dynamic interaction between the vehicle and the bridge is implemented in Matlab. The vehicle and the bridge are coupled at the tyre contact points via the interaction force vector, $\mathbf{f_{int}}$. Combining Eq. (1) and Eq. (9), the coupled equation of motion is formed as

$$\mathbf{M_g\ddot{u} + C_g\dot{u} + K_g u = F} \tag{13}$$

where $\mathbf{M_g}$ and $\mathbf{C_g}$ are the combined system mass and damping matrices respectively, $\mathbf{K_g}$ is the coupled time-varying system stiffness matrix and $\mathbf{F}$ is the system force vector. The vector, $\mathbf{u} = \{\mathbf{y_v}, \mathbf{y_b}\}^{\mathbf{T}}$ is the displacement vector of the system. The equations for the coupled system are solved using the Wilson-Theta integration scheme [22, 23]. The optimal value of the parameter θ = 1.420815 is used for unconditional stability in the integration schemes [24]. The scanning frequency used for all simulations is 1000 Hz.

3. Concept of Subtracting Axle Accelerations to Detect Bridge Damping

The vehicle is simulated travelling over a 100 m approach length followed by a 15 m simply supported bridge at 20 m s^{-1}. The Class 'A' road profile is generated according to ISO [25]. This is extrapolated into a number of different paths, where each path is correlated with the one next to it. Fig. 2 illustrates two paths through this road profile. The vehicle is simulated crossing each path separately to assess the sensitivity of the algorithm to transverse position of the vehicle. This is repeated six times, once for each level of damping (from 0% to 5%), representing different degrees of damage.

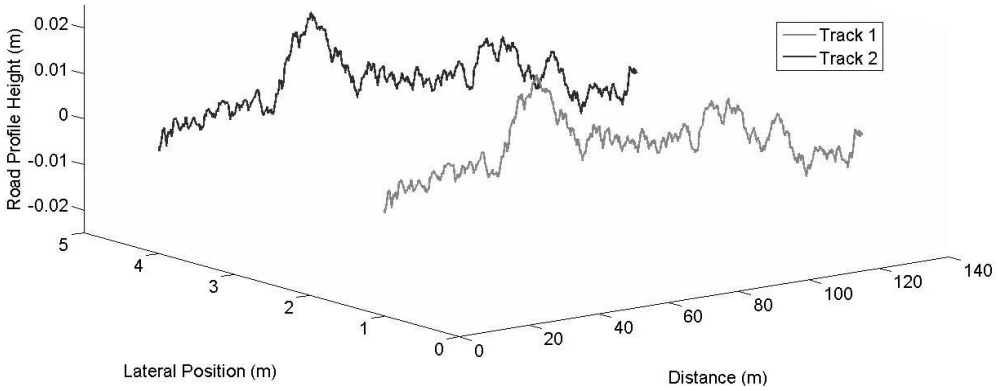

Fig. 2: Class 'A' Road Profile [25]

The trailer vertical accelerations are transformed from the time domain into the frequency domain using the Fast Fourier Transform. Plots of Power Spectral Density (PSD) against frequency can be seen in Fig. 3. In the PSD for an individual axle of the trailer (Fig. 3(a)), there is no peak corresponding to the bridge frequency (5.65 Hz) and there is no clear distinction between the different levels of damping (all six plots are on top of one another). The vibration of the vehicle dominates each spectrum. This is because the ratio of height of road irregularities to bridge displacements is too large for the bridge to have a significant influence on the vehicle.

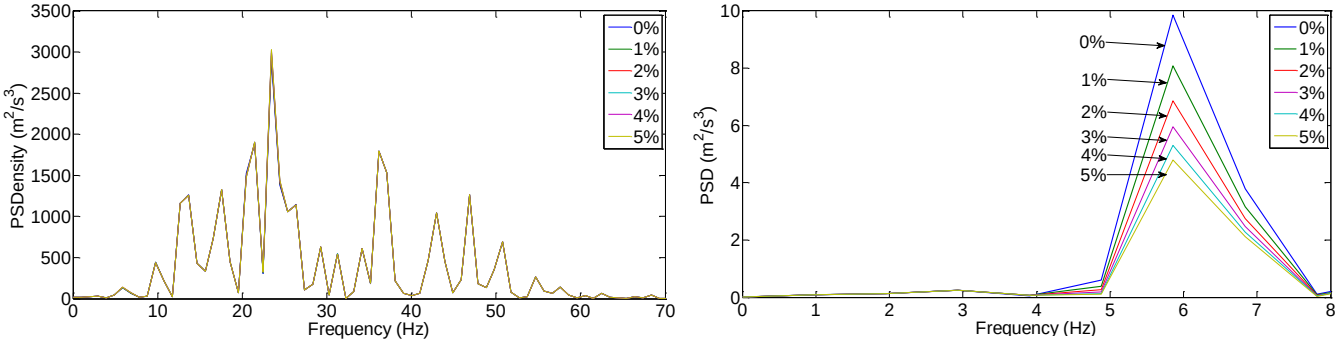

Fig. 3: PSD of Accelerations for Vehicle Travelling along Path 1 at 20 m s^{-1} over a 15 m Bridge; (a) Trailer Axle 1 Accelerations (b) Axle Acceleration Difference

However, when the trailer axle accelerations are subtracted from one another, allowing for the time shift, clear peaks become visible corresponding to the first natural frequency of the bridge, seen in Fig. 3(b). The first trailer axle is excited by the road profile and the bridge displacements as it passes each point on the bridge. The second trailer axle is excited by the same road profile and bridge displacements at different instants in time. The differences between the excitations include no element of road profile, only consisting of time lagged differences in bridge response. As such, this difference plot can be used to identify the influence of the bridge alone, without 'contamination' from the excitations due to road surface profile. It follows that the effect of bridge damping, hardly visible in Fig. 3(a), is clearly evident in Fig. 3(b). It is apparent from Fig. 3(b) that the magnitude of the peak decreases for higher levels of damping. This suggests that a truck-trailer vehicle system has the potential to be a practical method of detecting changes in PSD which then may be used as an indicator of changes in bridge damping. This same trend can be seen in Fig. 4(a) and Fig 4(b).

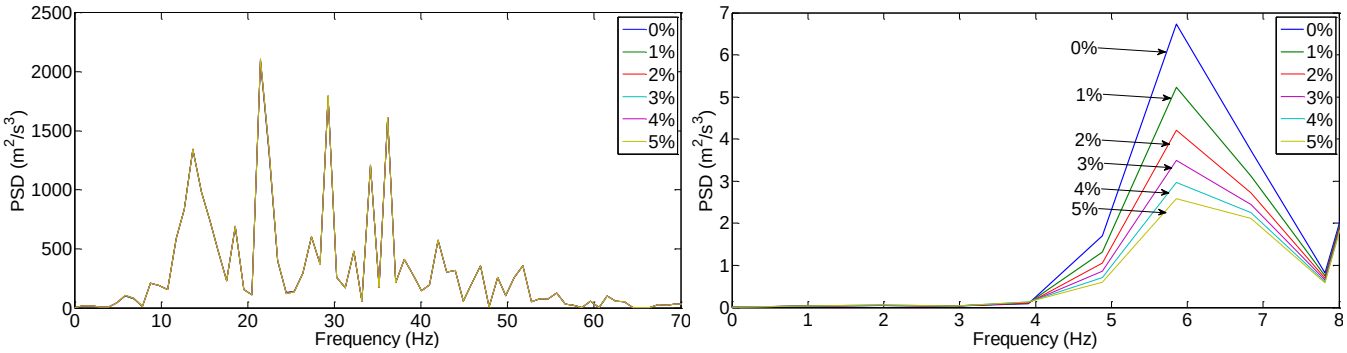

(a) (b)

Fig. 4: PSD of Accelerations for Vehicle Travelling along Path 2 at 20 m s^{-1} over a 15 m Bridge; (a) Trailer Axle 1 Accelerations (b) Axle Acceleration Difference

This illustrates that the method presented here is not sensitive to transverse position of the vehicle on the bridge. What can be noted, is that the magnitude of Power Spectral Density is larger for the second path (Fig. 4(b)) compared with the first path (Fig. 3(b)). This is due to the differing levels of excitation of the vehicle.

The PSD of the bridge mid span accelerations, which is the acceleration reading from instrumentation of the bridge as opposed to the vehicle, are also found. A peak occurs at 5.85 Hz here also. *This suggests that instrumentation of the vehicle can be of similar accuracy to results found by instrumenting the bridge.* There is a small difference between the frequencies that were predicted (5.65 Hz) and where the peak occurs (5.85 Hz) in Fig. 3 and Fig 4. The inaccuracy appears to be due to the spectral resolution (± 0.48 Hz), which can be improved by driving the vehicle at a slower speed.

4. Conclusions

This paper investigates the feasibility of using an instrumented truck-trailer vehicle model to monitor damping in a bridge. A method is presented that involves the subtraction of axle accelerations to remove much of the influence of the road profile. The results indicate that bridge frequency and changes in damping can be detected when the axle accelerations of the trailer are subtracted from one another. Results for the drive-by system are of similar quality to results for an accelerometer located on the bridge and the algorithm appears to be not sensitive to transverse position of the vehicle on the road.

5. Acknowledgements

The authors wish to express their gratitude for the financial support received from Science Foundation Ireland towards this investigation under the US-Ireland Research Partnership Scheme.

6. References

[1] J.M.W. Brownjohn, Structural health monitoring of civil infrastructure. Philosophical Transactions of the Royal Society A: Mathematical, Physical and Engineering Sciences 365 (2007) 589-622.

[2] P.C. Chang, A. Flatau, and S.C. Liu, Review paper: health monitoring of civil infrastructure. Structural Health Monitoring 2 (2003) 257-267.

[3] C.R. Farrar, K. Worden, An introduction to structural health monitoring. Philosophical Transactions of the Royal Society A: Mathematical, Physical and Engineering Sciences 365 (2007) 303-315.

[4] C.W. Kim, M. Kawatani, Challenge for a drive-by bridge inspection, Proceedings of the Tenth International Conference on Structural Safety and Reliability, Osaka, Japan, 2009, pp. 758-765.

[5] Y.B. Yang, C.W. Lin, J.D. Yau, Extracting bridge frequencies from the dynamic response of a passing vehicle. Journal of Sound and Vibration 272 (2004) 471-493.
[6] C.W. Lin, Y.B. Yang, Use of a passing vehicle to scan the fundamental bridge frequencies: An experimental verification. Engineering Structures 27 (2005) 1865-1878.
[7] Y.B. Yang, K.C. Chang, Extraction of bridge frequencies from the dynamic response of a passing vehicle enhanced by the EMD technique. Journal of Sound and Vibration 322 (2009) 718-739.
[8] Y. Oshima, T. Yamaguchi, Y. Kobayashi, K. Sugiura, Eigenfrequency estimation for bridges using the response of a passing vehicle with excitation system, Proceedings of the Fourth International Conference on Bridge Maintenance, Safety and Management, Seoul, Korea, (2008) pp. 3030-3037.
[9] T. Toshinami, M. Kawatani, C.W. Kim, Feasibility investigation for identifying bridge's fundamental frequencies from vehicle vibrations, Proceedings of the Fifth International Conference on Bridge Maintenance, Safety and Management, USA, (2010), pp. 317-322.
[10] F. Cerda, J. Garrett, J. Bielak, J. Barrera, Z. Zhuang, S. Chen, M. McCann, J. Kovačević, Indirect structural health monitoring in bridges: scale experiments, Proceedings of the Sixth International Conference for Bridge Maintenance and Safety, 2012, Stresa, Italy, pp. 346-353.
[11] A. Yabe, A. Miyamoto, Bridge condition assessment for short and medium span bridges by vibration responses of city bus, Proceedings of the Sixth International Conference for Bridge Maintenance and Safety, 2012, Stresa, Italy, pp. 195-202.
[12] C.W. Kim, R. Isemoto, K. Sugiura, M. Kawatani, Structural diagnosis of bridges using traffic-induced vibration measurements, Proceedings of the Sixth International Conference for Bridge Maintenance and Safety, 2012, Stresa, Italy, pp. 423-430.
[13] C. Williams and O.S. Salawu, Damping as a damage indication parameter, Proceedings of the 15th International Modal Analysis Conference, 1997, Orlando, Florida, USA, pp. 1531-1536.
[14] R.O. Curadelli, J.D. Riera, D. Ambrosini, M.G. Amani, Damage detection by means of structural damping identification. Engineering Structures 30 (2008) 3497-3504.
[15] C. Modena, D. Sonda, D. Zonta, Damage localization in reinforced concrete structures by using damping measurements. Key engineering materials 167 (1999) 132-141.
[16] P.J. McGetrick, A. González, E.J. OBrien, Theoretical investigation of the use of a moving vehicle to identify bridge dynamic parameters. Insight: Non-Destructive Testing & Condition Monitoring 51 (2009) 433-438.
[17] E.J. OBrien, Y. Li, and A. González, Bridge roughness index as an indicator of bridge dynamic amplification. Computers and Structures 84 (2006) 759-769.
[18] X.Q. Zhu, S.S. Law, Orthogonal Function in Moving Loads Identification in a Multi-span Bridge. Journal of Sound and Vibration 245 (2001) 329-345.
[19] DAF Trucks Limited, FAT CF75 30t Specification sheet, 2012.
[20] Y.B. Yang, J.D. Yau, Y.S. Wu, Vehicle-Bridge Interaction Dynamics: with Applications to High-Speed Railways, World Scientific Publishing Co. Pte. Ltd, Singapore, 2004.
[21] R.W. Clough, J. Penzien, Dynamics of structures, McGraw-Hill, 1975.
[22] K.J. Bathe, E.L. Wilson, Numerical methods in finite element analysis, Prentice-Hall, 1976.
[23] J.W. Tedesco, W.G. McDougal, C.A. Ross, Structural dynamics: theory and applications, Addison Wesley Longman, 1999.
[24] W. Weaver, P.R. Johnston, Structural dynamics by finite elements, Prentice-Hall, 1987.
[25] International Organisation for Standardisation ISO 8608, Mechanical vibration-road surface profiles - reporting of measured data, 1995.